CBM EXPERIMENT AT FAIR*

Paweł Staszel

for the CBM Collaboration

Institute of Physics, Jagellonian University
Reymonta 4, 30-059 Kraków, Poland

(Received January 5, 2010)

The Compressed Baryonic Matter (CBM) project at the future accelerator center FAIR will be a dedicated heavy-ion experimental operating in fixed target mode at beam energies from 8 to 45 A GeV. The ultimate goal of the research program is to explore the QCD phase diagram in the range of moderate temperature but the highest net-baryon densities. The CBM detector concept aims to obtain feasibility of measurement of hadronic, leptonic and photonic observables at interaction rates up to 10 MHz. It will allow to detect extremely rare probes such as charm near its production threshold. The CBM experiment will enter a new era with diagnostic probes never accessible before in the FAIR energy range, and thus has a unique research potential.

PACS numbers: 25.75.Dw

1. Introduction

In the last decades, collisions of heavy ions in the laboratory became an important tool for studying the phase diagram of strongly interacting matter. Depending on the incident energy a highly compressed baryon dominated system or an extremely hot mesonic phase is created in these collisions. Our knowledge about the evolution of baryon density *versus* collision energy is based both on theoretical and experimental arguments. A variety of models describing relativistic nucleus–nucleus reactions can predict the evolution of the net-baryon density with reaction time [1]. The models consistently show an increase of net-baryon density with increase of beam energy. For a beam energy of 30 A GeV they predict the net-baryon densities in the range from 2 to 3 fm^{-3} in the central reaction zone. From a statistical analysis of the final hadron yields measured in experiments from SIS to RHIC energies

* Presented at the XXXI Mazurian Lakes Conference on Physics, Piaski, Poland, August 30–September 6, 2009.

a chemical freeze-out curve has been established in the phase diagram [2]. At top RHIC energy which provides a measurement at baryo-chemical potential (μ_B) close to 25 MeV, the chemical freeze-out temperature is about 165 MeV. For top SPS and RHIC energies, *i.e.* at high T and low μ_B, indications were found pointing to the relevance of partonic degrees of freedom without having evidence of crossing a 1-st order phase transition. A novel representation of the chemical freeze-out curve in temperature (or energy density) *versus* net baryon density shows a well pronounced maximum in net-baryon density at beam energy around 30 A GeV [3].

The main research goal of the CBM project is to investigate the properties of strongly interacting matter in the range of high baryon density. The energy range of the future FAIR accelerator SIS100/300 will allow to create nuclear systems at temperatures of the order of 200 MeV and the highest experimentally achievable net-baryon densities. Quantum Chromodynamics (QCD), the theory that provides a fundamental description of the strong interaction, predicts several modifications of meson properties as a result of their interaction with a dense medium [4, 5]. The theory is still substantially evolving and the scientific progress in "strong" nonperturbative QCD is driven by new experimental data. The CBM experiment will allow to verify these predictions in the range of high baryon densities which are not accessible for present ultra-relativistic heavy ion experiments conducted at RHIC and at the Large Hadron Collider (LHC). In the ranges of thermodynamical variables (like *e.g.* temperature and baryon chemical potential) which are characteristic for the media created in the heavy ion reactions at SIS100/300, QCD predicts the existence of a 1st order phase boundary between hadronic and partonic phases and the critical end point. A delivery of experimental evidences for the predicted structures in the phase diagram together with mapping the in-medium properties of hadrons constitutes the main challenges for nuclear physics. Because of the unique beam intensities and a high precision measurement of various observables including rare probes, CBM is the most promising scientific enterprise among the present (NA61 at CERN) and the planned projects (STAR low energy scan program at BNL, NICA at Dubna).

2. Phase diagram and physics motivations

As it was mentioned, the statistical model analysis of particle yields measured in heavy-ion collisions at SIS, AGS, SPS and RHIC have been successfully used to describe the chemical freeze-out in nucleus–nucleus interactions. Some of these models show a remarkable behavior at low baryo-chemical potential where the curves of temperature *versus* baryo-chemical potential representing chemical freeze-out tend to merge with the phase boundary between partonic and hadronic media [2, 6]. In such a picture, hadrons are produced very close to freeze-out, and one could state that some features of the partonic medium can be transmitted to the final bulk hadrons via hadronization processes (see *e.g.* Fig. 3 in [7]). At higher μ_B however, the divergence of the two curves suggests the existence of a dense yet hadronic medium, which can be probed by nuclear collisions at beam energies between AGS and top SPS. Further insight into the dynamics of nucleus–nucleus collisions is obtained by hydrodynamical calculations [8] of the trajectories in the T–μ_B plane (see Fig. 1). According to these results, the deconfinement phase border is first reached around 10 A GeV beam energy; at 30 A GeV, the trajectory passes near the critical endpoint. At top SPS energy, the system evolves towards the low μ_B region of the phase diagram. These calculations suggest that phenomena connected with deconfinement as a result of a 1st order phase transition and the critical point are best studied using beam energies between AGS and top SPS energy. As it was argued above, in this energy range one can expect the formation of nuclear media at the highest net-baryon densities.

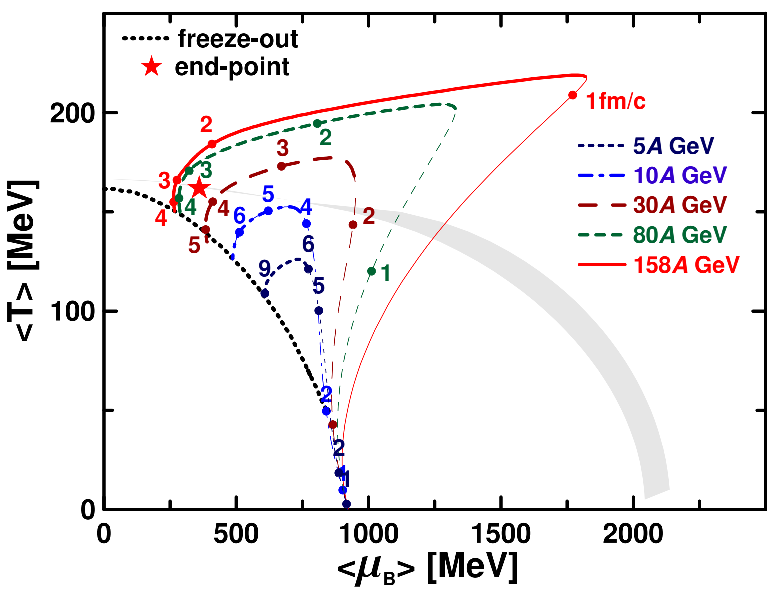

Fig. 1. Dynamical trajectories in the T–μ_B plane for central Pb+Pb collisions ($b = 2.5$ fm) at various incident energies. Numbers near the dynamical trajectories indicate the evolution time instants in the c.m. frame of the colliding nuclei. The light gray shaded region corresponds to the boundary of the phase transition from the hadronic phase to the QGP. The dotted line is the experimental freeze-out curve. The star symbol is the critical endpoint (see [8] for more details).

Several experimental observations reported by the NA49 experiment [9] indicate an onset of deconfinement at about 30 A GeV beam energy. Among these are the sharp peak in the relative strangeness content of the final state and the constant mean transverse momenta at SPS energies, which can be interpreted as signals of a first-order phase transition [10–12]. Although, the energy dependence of effective temperature in the kaon spectra from AGS to RHIC energies can be well reproduced for $p+p$ reactions by microscopic calculations using UrQMD and HSD models [13], the calculations fail in the description of central Au+Au and Pb+Pb data, significantly under-predicting the effective temperatures from kaon spectra. The introduction of 3-body collisions increases the inverse slope parameter of K^+ transverse mass spectra in central nucleus–nucleus reaction to an agreement within 10% (except for points in the energy range from 5.73 A GeV to top AGS energy) [14], however, the quality of data does not allow to draw final conclusions. Experimental signatures of the critical point, which should manifest in large dynamical event-by-event fluctuations have been sought for, but up to now, without conclusive results. In [15] a discussion of recent results together with model predictions for a critical point can be found. The properties of hadrons in a dense medium have also been topic of experimental and theoretical investigations. The excess of low-mass dielectrons observed by the CERES experiment in Pb+Pb collisions at 158 and 40 A GeV [16, 17] clearly advocates a strong in-medium modification of the spectral function, but the data quality does not allow to discriminate different in-medium scenarios. It turned out that the enhancement is about a factor of 2 larger at the lower energy, which indicates that the baryon density plays an important role in the observed phenomenon [18]. At the top SPS energy, high-quality data have been delivered by the NA60 experiment in the di-muon channel [19]. An enhancement by a factor of 4 in the mass range of 0.2–0.6 GeV/c^2 over the known hadronic sources has been found in central In+In collisions. The obtained spectral shape of the excess leptonic pairs contradicts the in-medium dropping mass scenario and is rather consisted with in-medium broadening of ρ and ω mesons [20]. The discovery of an anomalous suppression of the J/ψ at the top SPS energy was one of the major experimental results in the field of relativistic heavy ion reactions. Initially found by NA50 [22] and NA38 [21], the effect was confirmed by NA60 [23], that also shows that the anomalous suppression of the J/ψ scales with the number of participating nucleons ($N_{\rm part}$), thus is driven by the properties of the created medium. The suppression was initially attributed to charmonia dissociation in QGP, however a competitive hadronic scenario has been introduced by theory [5] and used to explain the data. It was namely, the in-medium decay of charmonia states into $D+\bar{D}$ pairs as a result of the reduction in the effective open charm meson mass due to its interaction with the dense medium. In [5] it was predicted that the mass reduction strongly increases with the increase of net-baryon density, thus lower energies are well suited for studying this effect.

Both the theoretical and experimental results outlined above motivate an experimental programme at lower beam energies involving a dedicated next-generation experiment for a comprehensive and systematic exploration of strongly interacting matter at high net-baryon densities.

3. The CBM detector concept

The experimental programme of CBM [24] comprises the measurements of

- short-lived light vector mesons (ρ, ω, ϕ) decaying into di-lepton pairs,
- baryons containing (anti) strange quarks, in particular the multi-strange $\mathit{\Lambda}, \mathit{\Xi}$ and $\mathit{\Omega}$ hyperos,
- mesons and baryons containing (anti) charm quarks, in particular J/ψ, D and $\mathit{\Lambda}_c$,
- direct photons,
- collective flow of all particles, event-by-event fluctuations of particle production.

All observables will be studied as a function of beam energy and system size, including the investigation of $p+p$, $p+A$, and $A+A$ collisions in the beam energy range from 8 to 45 A GeV (for ion beams with $Z/A = 0.5$) and up to 90 GeV for protons. In order to investigate rare probes as charm and di-leptons, up to 10 MHz interaction rate is foreseen. The high interaction rates require unprecedented detector performances in terms of speed and radiation hardness, as well as a fast and efficient on-line event selection. To cope with this requirements the core of the current detector concept (Fig. 2) will be a radiation hard silicon pixel/strip detector tracking system (STS) located inside a dipole field in order to provide high momentum resolution (1% for $p = 1\,\mathrm{GeV}/c$) and the reconstruction of secondary vertices with a precision of about $50\,\mu$m . Outside of the magnetic field, a RICH detector and several stations of transition radiation detectors (TRD) will identify electrons (with a pion suppression factor $\geq 10^4$) in the momentum ranges relevant for low-mass vector meson and charmonium measurements. In case vector mesons will be measured in their di-muon decay channel a set of absorber and detector layers will be placed instead of the RICH detector. Hadron identification will be achieved by the time-of-flight measurement in an array of resistive plate chambers (TOF) located 10 m from the target. The setup is completed by an electromagnetic calorimeter (ECAL) for identification of photons, electrons and neutral particles. Event characterization will be performed by a segmented projectile-spectator detector (PSD) located further downstream. The position information from the TRDs is used for global tracking through the detectors. Fig. 2 shows the layout of the planned experimental setup with detectors for electron identification.

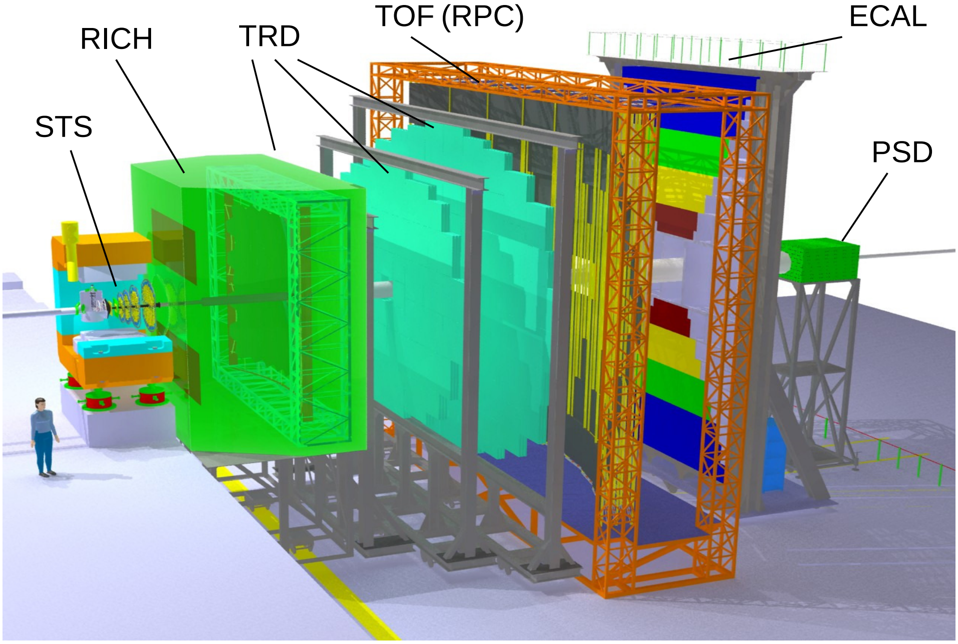

Fig. 2. Sketch of the CBM experiment with detectors for electron identification. The insert shows the location of the STS detection planes.

4. Feasibility studies

Progress in the preparation of the CBM experiment has been achieved with detailed feasibility studies, based on semi realistic implementations of the CBM detector systems and complete event reconstruction algorithms. These feasibility studies of the anticipated measurements serve also as a tool for the optimization of the detector setup.

4.1. Open charm

Due to the large charm quark mass, it is expected that charm is produced in the early stage of the collision. CBM will measure charm near the *pp* threshold, where the measured yield will be most sensitive to the conditions inside the dense fireball. The importance of the open charm measurement was already discussed in Sec. 2. The reconstruction of open charm mesons in the CBM experiment will be particularly challenging because about 800 charged particles are produced per central Au+Au collision at 25 A GeV beam energy in the polar angle range from 5° to 25° in the laboratory frame. In order to identify open charm mesons in their charged decay modes, *e.g.* $D^0 \rightarrow K^-\pi^+$ and $D^\pm \rightarrow \pi^\pm\pi^\pm K^\mp$, their decay vertices ($c\tau$ = 127 and 147 fm/c, respectively) have to be reconstructed with high precision. A good primary and secondary vertex resolution is thus the main handle for background reduction, moreover, the proton and kaon separation in the TOF detector allows for further reduction of the background. Placing two stations of micro vertex detectors (MVD), built from Monolithic Active Pixel Sensors [25] at 5 and 10 cm downstream the target, a secondary vertex resolution on the level of 50 μm can be achieved. The stations must be ultra-thin with a material budget corresponding to 0.3% and 0.5% of radiation lenght for the stations at 5 cm and 10 cm, respectively. The interaction rate is limited to 100 kHz as imposed by the maximum readout speed of the monolithic pixel detectors. With this MVD system, a data sample of about 7k D^0+ 20k $\bar{D}^0$ and 12k D^++ 26k D^- will be collected in 10 weeks of data taking with integrated efficiencies as shown in Fig. 3.

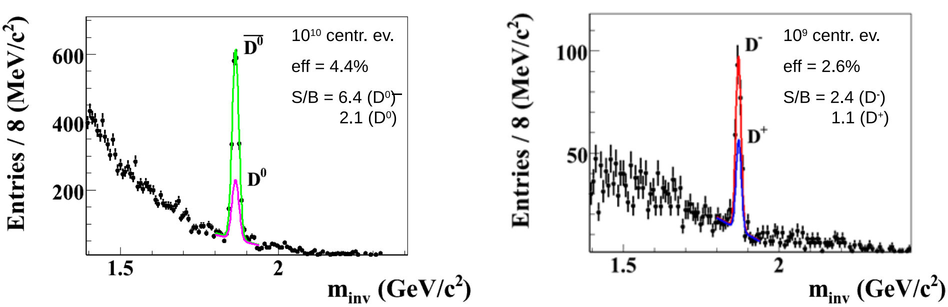

Fig. 3. Invariant mass spectra of reconstructed D mesons in central Au+Au collisions of 25 A GeV beam energy. The HSD [26] and UrQMD [27] models were used to generate signal and backgroud input, respectively.

4.2. Di-lepton spectroscopy

The feasibility of J/ψ and low-mass vector mesons measurements in CBM via their e^+e^- and $\mu^+\mu^-$ decay channels have been studied. The combined electron identification efficiency of RICH and TRD is about 85% at a π suppression factor of 10^4 for tracks with $p > 1$ GeV/c. The remaining background is dominated by π^0 Dalitz decays and γ-conversions in target and detector material. For the J/ψ measurement most of the background can be rejected requiring transverse momenta of the single electrons larger than 1.2 GeV/c. For the low-mass vector mesons, however, a sophisticated cut strategy making full use of the high tracking performance is being developed. The studies presented here were performed assuming a thin 25 μm Au target. Typical signal-to-background ratios and efficiencies for the low-mass vector mesons are 0.2 and 15% for the ω-meson and 0.5 and 23% for the ϕ-meson, respectively. Fig. 4 (left) shows the result of a J/ψ simulation in the di-electron channel for 10^{10} central Au+Au collisions at 25 A GeV beam energy. A signal-to-background ratio of 12 at a J/ψ reconstruction efficiency of 13% is achieved. For a J/ψ measurement in the di-muon channel a detector–absorber system (MUCH) is used. The device is composed of 6 absorbers with 5 gaps and 3 tracking detectors in each of the gaps. The total length of the absorbers is 2.25 m of iron which corresponds to 13.4 radiation length. The reconstruction of J/ψ in the di-muon channel provides high quality signals with a signal-to-background of the order 10 thus even putting the ψ' detection into reach. Fig. 4 (right) shows the invariant mass spectrum of reconstructed muon pairs in 10^{10} simulated central Au+Au collisions at 25 A GeV. The reconstruction efficiencies are similar to the electron channel (14%). Also a wide phase space acceptance is covered. A measurement of low mass vector mesons, however, suffers from the low momenta of their decay muons shifting the accessible phase space towards forward rapidities. In order to include soft muons only the first 1.25 m of iron absorber is required to be traversed. So far, in the di-muon channel, a signal-to-background ratio of 0.1 with a reconstruction efficiency of 2% for the ω-meson can be reached. Further investigations concentrate on improving the simulations including more and more realistic detector details and possible background sources.

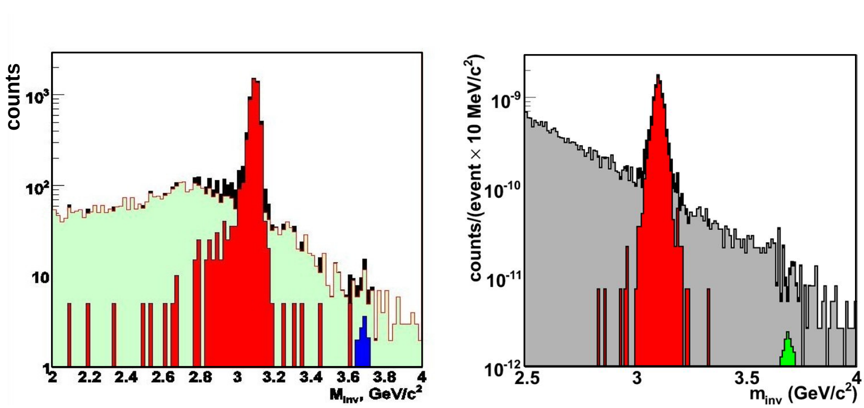

Fig. 4. Invariant mass spectrum for a J/ψ simulations in the electron (left) and muon channel (right). Both simulations include full event reconstruction for central Au+Au reactions at beam energy of 25 A GeV. The HSD [26] and UrQMD [27] models were used to generate signal and backgroud input, respectively.

4.3. Strangeness

Hadron identification is realized with the TOF system with 80 ps time resolution in 10 m distance from the target. Kaons can be identified up to momenta of $4\,\mathrm{GeV}/c$, with good phase space coverage and with an efficiency better than 80%. Hyperons can be identified via their decay topology in the STS system. The excellent tracking capability of the STS allows an almost background free reconstruction and high event statistics will enable CBM to measure not only spectra and yields, but also differential variables like flow. The strangenes excitation function will be a key measurement for the start version of CBM at SIS100 providing $A + A$ and $p + A$ collisions at beam energies up to $11\,A\,\mathrm{GeV}$ and $30\,\mathrm{GeV}$, respectively. Strange mesons are regarded as promising probes both for the study of the in-medium properties of hadrons and the nuclear equation-of-state at large baryon densities [28]. The measurement of multistrange hyperons such as Ξ and Ω which have not been observed below SPS energies will provide additional information on the role of strangeness at very high baryon densities.

5. Summary

The CBM experiment currently being planned at FAIR shows great physics discovery potential measuring new probes in the intermediate region of the QCD phase diagram at highest net-baryon densities. The experimental program will address topics like the onset of deconfinement, the search for a 1st order phase transition and the critical point, and in-medium properties of hadrons. Detailed excitation functions of even rarely produced hadrons as D-mesons, charmonia states and multistrange hyperons will be investigated in heavy ion collisions at energies from 8 to $45\,A\,\mathrm{GeV}$ beam energy. This ability presents a unique feature of CBM among other, present and future experimental projects that at this energy range have access only to the bulk observables. Feasibility studies have shown that the measurements of the key observables with the planned detector setup are feasible. They, require, however the development of new, fast radiation hard detectors as well as on-line event reconstruction with unprecedented speed. R&D is under way for all detector components facing the challenge of the foreseen high interaction rates. Starting from 2016, CBM should thus be able to deliver highly interesting data improving the understanding of high baryon density matter.

REFERENCES

[1] I.C. Arsene *at al., Phys. Rev.* **C75**, 034902 (2007) and references therein.

[2] A. Andronic, P. Braun-Munzinger, J. Stachel, *Nucl. Phys.* **A772**, 167 (2006).

[3] J. Randrup, J. Cleymans, *Phys. Rev.* **C74**, 047901 (2006).

[4] R. Rapp, J. Wambach, *Adv. Nucl. Phys.* **25**, 1 (2000).

[5] A. Mishra, E.L. Bratkovskaya, J. Shaffer-Bielich, S. Schramm, H. Stöcker, *Phys. Rev.* **C69**, 015202 (2004).

[6] P. Braun-Munzinger, *Nucl. Phys.* **A681**, 119c (2001).

[7] A. Andronic, P. Braun-Munzinger, J. Stachel, `arXiv:09114931[nucl-th]`.

[8] Yu.B. Ivanov, V.N. Russkikh, V.D. Toneev, *Phys. Rev.* **C73**, 044904 (2006).

[9] M. Gaździcki for the NA49 Collaboration, *J. Phys. G* **30**, S701 (2004).

[10] M. Gaździcki, M.I. Gorenstein, *Acta Phys. Pol. B* **30**, 2705 (1999).

[11] M.I. Gorenstain, M. Gaździcki, K.A. Bugaev, *Phys. Lett.* **B567**, 175 (2003).

[12] M. Gaździcki *at al., Braz. J. Phys.* **34**, 322 (2004).

[13] E. Bratkovskaya *et al., Phys. Rev. Lett.* **92**, 032302 (2004).

[14] A.B. Larionov, O. Buss, K. Gallmeister, U. Mosel, *Phys. Rev.* **C76**, 044909 (2007).

[15] [NA49 Collaboration] K. Grebieszkow *et al.*, `arXiv:0907.4101` and references therein.

[16] [CERES Collaboration] B. Lenkeit, *Nucl. Phys.* **A661**, 23c (1999).

[17] D. Adamová *et al., Phys. Rev. Lett.* **91**, 042301 (2003).

[18] R. Rapp, J. Wambach, *Eur. Phys. J.* **A6**, 415 (1999).

[19] [NA60 Collaboration] R. Arnaldi *et al., Phys. Rev. Lett.* **96**, 162302 (2006); [NA60 Collaboration] R. Arnaldi *et al., Phys. Rev. Lett.* **100**, 022302 (2008).

[20] J. Ruppert, C. Gale, T. Renk, P. Lichard, J.I. Kapusta, *Phys. Rev. Lett.* **100**, 162301 (2008).

[21] [NA38 and NA50 Collaboration] M.C. Abreu *et al., Eur. Phys. J.* **C14**, 443 (2000).

[22] [NA50 Collaboration] B. Borges *et al., Eur. Phys. J.* **C34**, 161 (2005).

[23] [NA60 Collaboration] R. Arnaldi *et al., Phys. Rev. Lett.* **99**, 132302 (2007); [NA60 Collaboration] E. Scomparin, *Nucl. Phys.* **A774**, 67 (2006).

[24] [CBM Collaboration], *Letter of Intent for the Compressed Baryonic Matter Experiment*, Darmstadt 2004 `[http://www.gsi.de/documents/DOC-2004-Mar-105.html]`.

[25] M. Deveaux *et al., PoS* **VERTEX**, 28 (2008).

[26] W. Cassing, E.L. Brathovskaya, *Phys. Rep.* **308**, 65 (1999).

[27] M. Bleicher *et al., J. Phys. G* **25**, 1859 (1999).

[28] P. Senger, *Nucl. Phys.* **A804**, 274 (2008).